



# Investigating the Implications of *CFTR* Exon Skipping Using a *Cftr* Exon 9 Deleted Mouse Model

Kelly M. Martinovich<sup>1,2,3</sup>, Anthony Kicic<sup>1,2,4,5,6</sup>, Stephen M. Stick<sup>1,2,4,5</sup>, Russell D. Johnsen<sup>3,7</sup>, Sue Fletcher<sup>3,7,8</sup> and Steve D. Wilton<sup>3,7\*</sup>

<sup>1</sup>School of Medicine, The University of Western Australia, Perth, WA, Australia, <sup>2</sup>Telethon Kids Institute, Wal-yan Respiratory Research Centre, Perth, WA, Australia, <sup>3</sup>Centre for Molecular Medicine and Innovative Therapeutics, Health Futures Institute, Murdoch University, Murdoch, WA, Australia, <sup>4</sup>Centre for Cell Therapy and Regenerative Medicine, School of Medicine and Pharmacology, The University of Western Australia, Perth, WA, Australia, <sup>5</sup>Department of Respiratory and Sleep Medicine, Perth Childrens Hospital, Nedlands, WA, Australia, <sup>6</sup>School of Population Health, Curtin University, Bentley, WA, Australia, <sup>7</sup>Perron Institute for Neurological and Translational Sciences, Centre for Neuromuscular and Neurological Disorders, The University of Western Australia, Nedlands, WA, Australia, <sup>8</sup>PYC Therapeutics, Perth, WA, Australia

## OPEN ACCESS

### Edited by:

Lezanne Ooi,  
University of Wollongong, Australia

### Reviewed by:

Onofrio Laselva,  
University of Foggia, Italy  
Leah Reznikov,  
University of Florida, United States

### \*Correspondence:

Steve D. Wilton  
S.Wilton@murdoch.edu.au

### Specialty section:

This article was submitted to  
Pharmacology of Ion Channels and  
Channelopathies,  
a section of the journal  
Frontiers in Pharmacology

Received: 03 February 2022

Accepted: 07 March 2022

Published: 22 March 2022

### Citation:

Martinovich KM, Kicic A, Stick SM, Johnsen RD, Fletcher S and Wilton SD (2022) Investigating the Implications of *CFTR* Exon Skipping Using a *Cftr* Exon 9 Deleted Mouse Model. *Front. Pharmacol.* 13:868863. doi: 10.3389/fphar.2022.868863

**Introduction:** Severity and disease progression in people with Cystic Fibrosis (CF) is typically dependent on their genotype. One potential therapeutic strategy for people with specific mutations is exon skipping with antisense oligonucleotides (AO). *CFTR* exon 9 is an in-frame exon and hence the exclusion of this exon would excise only 31 amino acids but not alter the reading frame of the remaining mRNA. Splice mutations 1209 + 1 G > C and 1209 + 2 T > G were documented to cause *CFTR* exon 9 skipping and these variants were reported to manifest as a milder CF disease, therefore exon 9 skipping could be beneficial for people with class I mutations that affect exon 9 such as p.Trp401X. While the impact of exon 9 skipping on gene expression and cellular pathways can be studied in cells *in vitro*, trace amount of full-length normal or mutated material could confound the evaluation. To overcome this limitation, the impact of *CFTR* exon 9 skipping on disease phenotype and severity is more effectively evaluated in a small animal model. It was hypothesised that antisense oligonucleotide-mediated skipping this particular exon could result in a “mild mouse CF phenotype”.

**Methods:** *Cftr* exon 9 deleted mice were generated using homologous recombination. Survival of homozygous (*Cftr*<sup>Δ9/Δ9</sup>) and heterozygous (*Cftr*<sup>Δ9/+</sup>) mice was compared to that of other CF mouse models, and lung and intestinal organ histology examined for any pathologies. Primary airway epithelial cells (pAECs) were harvested from *Cftr*<sup>Δ9/Δ9</sup> mice and cultured at the Air Liquid Interface for *CFTR* functional assessment using Ussing Chamber analysis.

**Results:** A *Cftr*<sup>Δ9/Δ9</sup> mouse model presented with intestinal obstructions, and at time of weaning (21 days). *Cftr*<sup>Δ9/Δ9</sup> mice had a survival rate of 83% that dropped to 38% by day 50. Histological sections of the small intestine from *Cftr*<sup>Δ9/Δ9</sup> mice showed more goblet cells and mucus accumulation than samples from the *Cftr*<sup>Δ9/+</sup> littermates. Airway epithelial cell cultures established from *Cftr*<sup>Δ9/Δ9</sup> mice were not responsive to forskolin stimulation.

**Summary:** The effect of *Cftr* exon 9 deletion on Cftr function was assessed and it was determined that the encoded Cftr isoform did not result in a milder “mouse CF disease phenotype,” suggesting that *Cftr* exon 9 is not dispensable, although further investigation in human CF pAECs would be required to confirm this observation.

**Keywords:** mouse model, cystic fibrosis transmembrane conductance regulator, exon skipping therapy, transgenic mouse, exon deletion

## INTRODUCTION

Severity and disease progression in people with Cystic Fibrosis (CF) is typically dependent on their genotype. One personalised therapeutic option is the use of exon skipping antisense oligonucleotides (AO) that are based on a specific genotype (Radpour et al., 2007; Shteinberg et al., 2017; Gaikwad et al., 2018). A review of the literature led to two observations that have suggested partial redundancy of *CFTR* exon 9: 1) splice mutations 1209 + 1 G > C and 1209 + 2 T > G were documented to cause *CFTR* exon 9 skipping and these variants were reported to manifest as a milder form of disease caused by mutations in the *CFTR* gene; congenital bilateral absence of vas deferens (CBAVD) (Li et al., 2012) and 2) *CFTR* exon 9 is in-frame and is reported to carry relatively few CF-causing mutations, when compared to other *CFTR* exons (Toronto 2011; Henrie et al., 2018; Molinski et al., 2018). *CFTR* exon 9 is an in-frame exon therefore the exclusion of this exon would not alter the reading frame of the remaining mRNA. This strategy could be beneficial for people with class I “null mutations” in exon 9 such as p.Trp401X that prevent synthesis of a functional protein. While the impact of exon 9 skipping on gene expression and cellular pathways can be studied in cells *in vitro*, trace amounts of full-length normal or mutated material could confound the testing. To overcome this limitation, the impact of *CFTR* exon 9 skipping on disease phenotype and severity should be more effectively evaluated in a small animal model.

Typically, mice homozygous for a *Cftr* mutation or disrupted *Cftr* gene display many features common to a young person with CF caused by two severe mutations (ie p.Phe508del), including failure to thrive, meconium ileus, alteration of mucus and serous glands, and obstruction of gland-like structures with thickened eosinophilic material (Lavelle et al., 2016). Genetically modified mouse models of CF disease were initially created by homologous recombination in embryonic stem cells through targeting a mutation to a specific site in the murine genome, each with varied outcomes (Clarke et al., 1994; Gosselin et al., 1998) (Davidson and Rolfe 2001). (Davidson and Rolfe 2001). Typically, CF-associated death in mouse models with specific *Cftr* mutations was from intestinal obstruction, usually before 40 days of age (Snouwaert et al., 1992). Some CF mouse models used gene insertions without loss of genomic sequence therefore, potentially allowing a small amount of normal *Cftr* mRNA to be expressed that may contribute to a reduced severity of disease (Davidson and Rolfe 2001; Scholte et al., 2004). There are ‘two residual function’ CF mouse models, *Cftr*<sup>tm/Hgu</sup> and *Cftr*<sup>tm/Bay</sup> that show 90 and 40% survival respectively, but also have 10 and 2% of wild type (WT) *Cftr* mRNA present that would contribute

to their higher survival rates (O’Neal et al., 1993; Wilke et al., 2011). Furthermore, three mouse models with the p.Phe508del mutation exist, showing variable WT CFTR mRNA levels and survival rates (5–90% survival at weaning) (Colledge et al., 1995; Zeiher et al., 1995; Rozmahel et al., 1996; Davidson and Rolfe, 2001).

Some transgenic CF mouse models used a gene replacement strategy to disrupt the *Cftr* gene creating absolute nulls. These complete *Cftr* KO models have no WT mRNA detected, such as *Cftr*<sup>tm/Unc</sup>; *Cftr*<sup>tm/Cam</sup>; *Cftr*<sup>tm/Hsc</sup>; *Cftr*<sup>tm3Bay</sup>; *Cftr*<sup>tm3Uth</sup> and have also shown variable survival rates after weaning (5–40%) (Colledge et al., 1995). *Cftr* mouse models generated with various mutations that result in nonsense mediated decay led to an absence of the functional Cftr protein (Snouwaert et al., 1992; O’Neal et al., 1993; Ratcliff et al., 1993; Hasty et al., 1995; Rozmahel et al., 1996; Wilke et al., 2011). One of these CF KO mouse models was generated with a premature termination codon in *Cftr* exon 2 (*Cftr*<sup>m3/Bay</sup>) and resulted in intestinal obstruction, which led to death in 60% of the mutant animals within 1 month after birth (Hasty et al., 1995).

The β-ENaC mouse model was the first to recapitulate the pathophysiology of the CF lung. This model over-expresses the β subunit of the ENaC with increased sodium ion absorption. Mice present with reduced airway surface liquid, reduced mucociliary clearance with airway mucus obstruction, goblet cell hyperplasia, chronic lung inflammation, and high mortality related to the lung disease (Zhou et al., 2011). Although these differences reinforce the notion that mouse models do not accurately recapitulate the human disease phenotype or progression, they can provide important mechanistic data.

We hypothesised that *CFTR* exon 9 could be partially redundant, meaning the encoded amino acids might not be essential for full CFTR function, therefore enabling an exon skipping AO strategy to be therapeutic for people with amenable mutations in that exon. Skipping of *CFTR* exon 9 would not disrupt the reading frame and if the resultant isoform retained some function, that could result in a “milder mouse CF phenotype” when compared to complete KO models. To investigate this possibility, a *Cftr* exon 9 deleted mouse model (*Cftr*<sup>Δ9/Δ9</sup>) was generated using homologous recombination that has no residual WT mRNA. Survival rates were compared to other CF mouse models and lung and intestinal organ histology examined for any pathologies. Primary airway epithelial cells (pAECs) were also harvested from *Cftr*<sup>Δ9/Δ9</sup> mice and cultured at the air liquid interface (ALI) for CFTR functional assessment using Ussing Chamber analysis.

## METHODS

### Generation of *Cftr*<sup>Δ9/Δ9</sup> Mouse Model

The *Cftr*<sup>Δ9/Δ9</sup> mouse line was generated by Ozgene Pty Ltd. (Bentley WA, Australia) and approved by Murdoch University Animal ethics committee (Protocol ID: R3109/19). The targeting construct was electroporated into a C57BL/6 embryonic stem cell line, *Bruce4* (Koentgen et al., 2016). Homologous recombinant embryonic stem cell clones were identified by quantitative PCR and injected into goGermline blastocysts (Ozgene) (Koentgen et al., 2016). Male chimeric mice were obtained and crossed to C57BL/6J females to establish heterozygous germline offspring on the C57BL/6 background. The germline mice were crossed to a ubiquitous Cre C57BL/6 mouse line to remove the loxP flanked sequence. *Cftr*<sup>Δ9/Δ9</sup> were generated through heterozygous breeding and pups were genotyped at birth. Since feed and housing conditions have been documented to influence the survival of CF mouse models (Snouwaert et al., 1992; Cottart et al., 2007), after weaning (21 day) *Cftr*<sup>Δ9/Δ9</sup> mice were fed exclusively with Peptamen® (Nestle Health Science) 1 kcal/ml peptide based liquid feed to prevent gastrointestinal occlusions (Snouwaert et al., 1992). All mice were housed on ALPHA-dri® bedding (Shepherd Specialty Papers). Mice were monitored as per routine husbandry guidelines for up to 150 days and if euthanasia was required before 150 days due to intestinal obstruction or malnutrition, tracheas were harvested for pAEC cultures and lungs, intestines, heart, kidneys and liver were fixed in 4% paraformaldehyde (Sigma-Aldrich). Euthanasia was done by inhaled anaesthetic followed by cervical dislocation. Mice were not routinely weighed.

### Histology

Organs such as the lungs, intestines, heart, kidneys and liver were fixed in 4% paraformaldehyde and were removed from fixative and placed in a standard histology cassette for processing. After overnight dehydration, tissue blocks were processed for paraffin embedding using a Leica tissue processor. After processing, specimens were placed into the embedding station wash bath. Sections (5 μm) were cut using the Leica RM2125 RTS The Essential Microtome (Leica Biosystems) and allowed to bake at 60°C for 30 min, after which they were stained with Hematoxylin and Eosin (H & E) (Sigma-Aldrich) or Alcian Blue (Sigma-Aldrich) using a Leica Autostainer and visualised using an Olympus BX53 microscope with DP72 camera and images captured using NIS-Elements software.

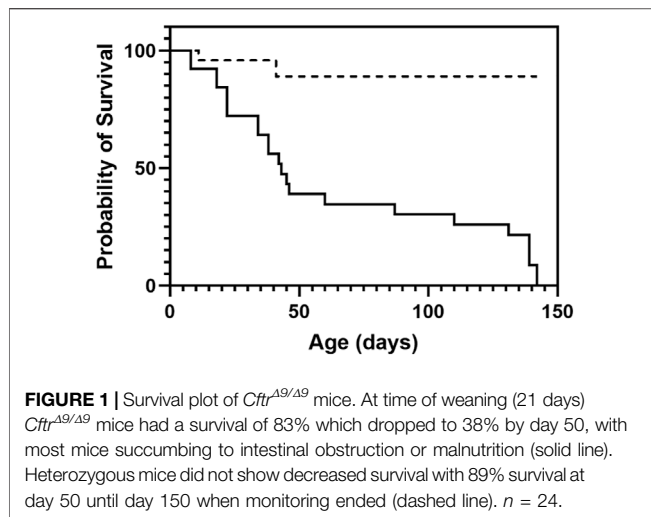
### Mouse Airway Epithelial Cell Collection

Tracheas were harvested and digested in 1.5 mg/ml pronase as previously described (Lam et al., 2011). Briefly, tracheas were harvested from mice and placed into 30 ml of Ham's F12 medium 1% penicillin/streptomycin and 1% fungizone and transferred to a sterile laminar flow hood. Tracheas were then cut along the vertical axis to expose the lumen and transferred to a new 50 ml tube containing 10 ml of Hams's F12 medium (GIBCO) with antibiotics and 1.5 mg/ml pronase and incubated on a roller at 4°C overnight. The following day, 10 ml of Ham's F12 medium

containing 20% FBS and antibiotics were added, and the tube inverted 12 times. Three tubes containing Ham's F12 medium, 20% FBS and antibiotics were prepared, and tracheas transferred to the first tube and then inverted 12 times and repeated twice more before the remaining tissue was discarded. All solutions were then combined and centrifuged at 1,400 rpm for 10 min at 4°C. The cell pellet was resuspended in 1 ml of DNase solution containing 10 mg/ml BSA, 10 mg/ml DNase I (Roche) made up in Hams's F12 medium containing antibiotics and incubated for 5 min on ice. Cells were then centrifuged at 1,400 rpm for 10 min at 4°C, resuspended in mouse tracheobronchial epithelial cell (MTEC) medium containing 10% FBS and plated into a plastic tissue culture dish before incubation at 37°C, 95% air, 5% CO<sub>2</sub> for 5 h to negatively select fibroblasts (Lam et al., 2011). Afterwards, the supernatant was collected, and the dish was rinsed with 4 ml of MTEC medium containing 10% FBS, that was then pooled with the supernatant and centrifuged at 1,400 rpm for 10 min at 4°C. Cell pellets were then resuspended for appropriate primary cell culture seeding.

### Mouse Airway Epithelial Cell Culture and Functional CFTR Assessment

For monolayer epithelial cells cultures, harvested tracheal cells were resuspended in 4 ml MTEC basic media (Lam et al., 2011) and plated into 6 well plates, precoated with 50 μg/ml collagen I and incubated at 37°C, in 95% air, 5% CO<sub>2</sub>. Once confluent, cells were trypsinised using the ReagentPack™ Subculture Reagents (Lonza™) according to the manufacturer's instructions. Cells were then centrifuged at 1,400 rpm for 10 min at 4°C before the pellet was resuspended in 1 ml of MTEC proliferation media (Lam et al., 2011) and a total cell count performed. Cells (300,000) were seeded into collagen I pre-coated apical compartments of a Corning® Costar® 12 mm Snapwell™ cell culture insert with 0.4 μm pore polycarbonate membrane (3,407 Sigma), as previously described (Martinovich et al., 2017). To complete the culture, 2 ml of MTEC proliferation medium was added to the basolateral compartment and cultures incubated at 37°C, 95% air, 5% CO<sub>2</sub>. Cultures were monitored and media replaced daily. Once cells were confluent, the apical compartment media was removed and not replaced, exposing the insert to air, creating an air liquid interface (ALI) and allowing the cells to fully differentiate. Once airlifted, the basolateral MTEC proliferation media was supplemented with 2% v/v Ultrosor™ G serum substitute (15,950-017 Pall) and 0.1 μM Trans-retinoic acid and changed every second day. To monitor monolayer differentiation transepithelial electrical resistance (TEER) measurements were performed twice weekly with STX2 chopstick electrodes and Epithelial Voltohmmeter EVOM<sup>2</sup> (World Precision Instruments). Ussing chamber (Physiologic Instruments Inc.) analysis was performed on day 28 post ALI, as previously described (Martinovich et al., 2017). Briefly, A chloride ion gradient was established by filling the basolateral compartment with Krebs Ringer bicarbonate solution as previously described (Thomas et al., 2000). Chambers were manipulated with Amiloride (50 μM Sigma-Aldrich), Forskolin (0.2–20 μM F6886 Sigma-Aldrich), CFTR-inhibitor 172 (30 μM



219,670 Sigma-Aldrich) and Ivacaftor (3  $\mu$ M VX-770, Selleckchem). Inserts were pre-treated with either Lumacaftor (3  $\mu$ M VX-809, Selleckchem) or DMSO (0.001%, Sigma-Aldrich) 24 h prior to Ussing Chamber analysis. Tracings were recorded using Acquire and Analyse 2.3 software (Physiologic Instruments Inc.) and raw values exported to excel. The short circuit current (Isc) data was then visualised using GraphPad Prism 8 software. For magnitude of change in Isc due to drug manipulations, the stable values immediately before and after the change were recorded and the differences plotted using GraphPad Prism 8 software.

## RESULTS

### *Cftr*<sup>Δ9/Δ9</sup> Mice

*Cftr*<sup>Δ9/Δ9</sup> pups were successfully generated from heterozygous breeding that resulted in 107 pups (12%) that were *Cftr*<sup>Δ9/Δ9</sup>, 31% *Cftr*<sup>+/+</sup> and 57% *Cftr*<sup>Δ9/+</sup>. Homozygous *Cftr*<sup>Δ9/Δ9</sup> pups were supplied with Peptamen food at approximately day 14 and weaned around day 21. At time of weaning (21 days) *Cftr*<sup>Δ9/Δ9</sup> mice had a survival rate of 83%. By day 50, more than half of the *Cftr*<sup>Δ9/Δ9</sup> mice had signs of intestinal obstruction or malnutrition and were humanely euthanised (**Figure 1**) compared to the 89% event free survival rate of the *Cftr*<sup>Δ9/+</sup> littermates (*n* = 24, 14 Male and 10 Female). Mice were not routinely weighed, however *Cftr*<sup>Δ9/Δ9</sup> mice were noted to have a “scruffier” appearance and “a general failure to thrive” by Ozgene staff members who were maintaining the colony.

To identify any pathological changes in the lungs of the *Cftr*<sup>Δ9/Δ9</sup> mice, the lungs were excised and prepared for histology and H & E staining (*n* = 4/group, 2 Male and 2 Female/group). The age of the mice at time of collection varied, dependant on when the *Cftr*<sup>Δ9/Δ9</sup> animals met the humane endpoint and ranged from 21 to 150 days of age, with *Cftr*<sup>Δ9/+</sup> mice age matched where possible. Upon examination, no obvious lung fibrosis or mucus accumulation was evident in the homozygous *Cftr*<sup>Δ9/Δ9</sup> lungs or their *Cftr*<sup>Δ9/+</sup> littermates (**Figures**

**2A,B**). Macroscopic examination showed homozygous *Cftr*<sup>Δ9/Δ9</sup> mice had intestinal obstruction to some degree at the time of euthanasia. Intestinal blockages appeared to be composed of an inspissated mixture of food material and possibly mucus, with considerable distention of the intestine observed proximally to the blockages. Histologically, some of the *Cftr*<sup>Δ9/Δ9</sup> mouse intestine sections showed distention with large luminal space, with no other obvious abnormalities (**Figures 2C,D**). The small intestine sections from *Cftr*<sup>Δ9/Δ9</sup> mice showed that the crypts of Lieberkühn were dilated (**Figure 2E**), compared with those from the *Cftr*<sup>Δ9/+</sup> litter mates (**Figure 2F**). There were no differences between genders.

Alcian blue stains mucus a bright blue and staining of organ sections revealed that crypts of Lieberkühn in *Cftr*<sup>Δ9/Δ9</sup> mice contained mucus, however, this did not differ to that of the *Cftr*<sup>Δ9/+</sup> control mice (**Figures 2G,H**). *Cftr*<sup>Δ9/Δ9</sup> did appear to have more goblet cells (**Figures 2I,J**) than their *Cftr*<sup>Δ9/+</sup> littermates, however this was not quantified. No macroscopic abnormalities were noted in the spleen, kidneys or liver. Due to the relatively small colony size generated in this study, quantification of goblet cell number or the characterisation of mucus accumulation could not be performed.

### *Cftr*<sup>Δ9/Δ9</sup> Airway Epithelial Cells

Primary airway cultures from *Cftr*<sup>Δ9/Δ9</sup> deleted mice exhibited typical epithelial cobblestone morphology when grown as a submerged monolayer (**Figure 3A**, *n* = 4). *Cftr*<sup>Δ9/+</sup> littermates failed to culture due to contamination, poor cellular adherence to the culture surface therefore this control group is lacking. When grown at the ALI, the *Cftr*<sup>Δ9/Δ9</sup> pAECs were densely packed with beating cilia (**Figure 3B**), typical of a pseudostratified mucociliary differentiated culture insert. To assess differentiation, TEER of ALI culture inserts was measured, peaking on day 9 at ~ 3,100  $\Omega$ /cm<sup>2</sup>. As differentiation progressed, the TEER dropped to ~ 700  $\Omega$ /cm<sup>2</sup> on day 18 and was maintained until Ussing chamber analysis was conducted on day 28 (Martinovich et al., 2017). Primary *Cftr*<sup>Δ9/Δ9</sup> ALI cultures were pre-treated with either a DMSO control (**Figures 4A,B**) or Lumacaftor (**Figures 4C,D**) for 24 h before routine CFTR functional analysis using an Ussing chamber. All *Cftr*<sup>Δ9/Δ9</sup> ALI cultures demonstrated a drop in short circuit current (Isc) in response to amiloride addition, representing the blocking of sodium adsorption (DMSO:  $-16.5 \pm 9.2 \mu\text{A}/\text{cm}^2$ , Lumacaftor:  $-19.9 \pm 1.061 \mu\text{A}/\text{cm}^2$ , *n* = 2). In addition, *Cftr*<sup>Δ9/Δ9</sup> ALI cultures showed a very minimal response to forskolin stimulation (DMSO:  $-0.5 \pm 0.6 \mu\text{A}/\text{cm}^2$ , Lumacaftor:  $-1.4 \pm 0.8 \mu\text{A}/\text{cm}^2$ , *n* = 2), negative response to Ivacaftor (DMSO:  $-2.6 \pm 3.9 \mu\text{A}/\text{cm}^2$ , Lumacaftor:  $-0.5 \pm 0.1 \mu\text{A}/\text{cm}^2$ , *n* = 2) and minimal response to CFTR inhibitor-172 (DMSO:  $-1.8 \pm 1.1 \mu\text{A}/\text{cm}^2$ , Lumacaftor:  $-1.3 \pm 1.1 \mu\text{A}/\text{cm}^2$ , *n* = 2) (**Figure 4E**).

## DISCUSSION

Here, the literature was interrogated for an exon that harboured multiple CFTR mutations that presented as a milder form of CF disease (ie CBAVD) indicating that the exon could be partially

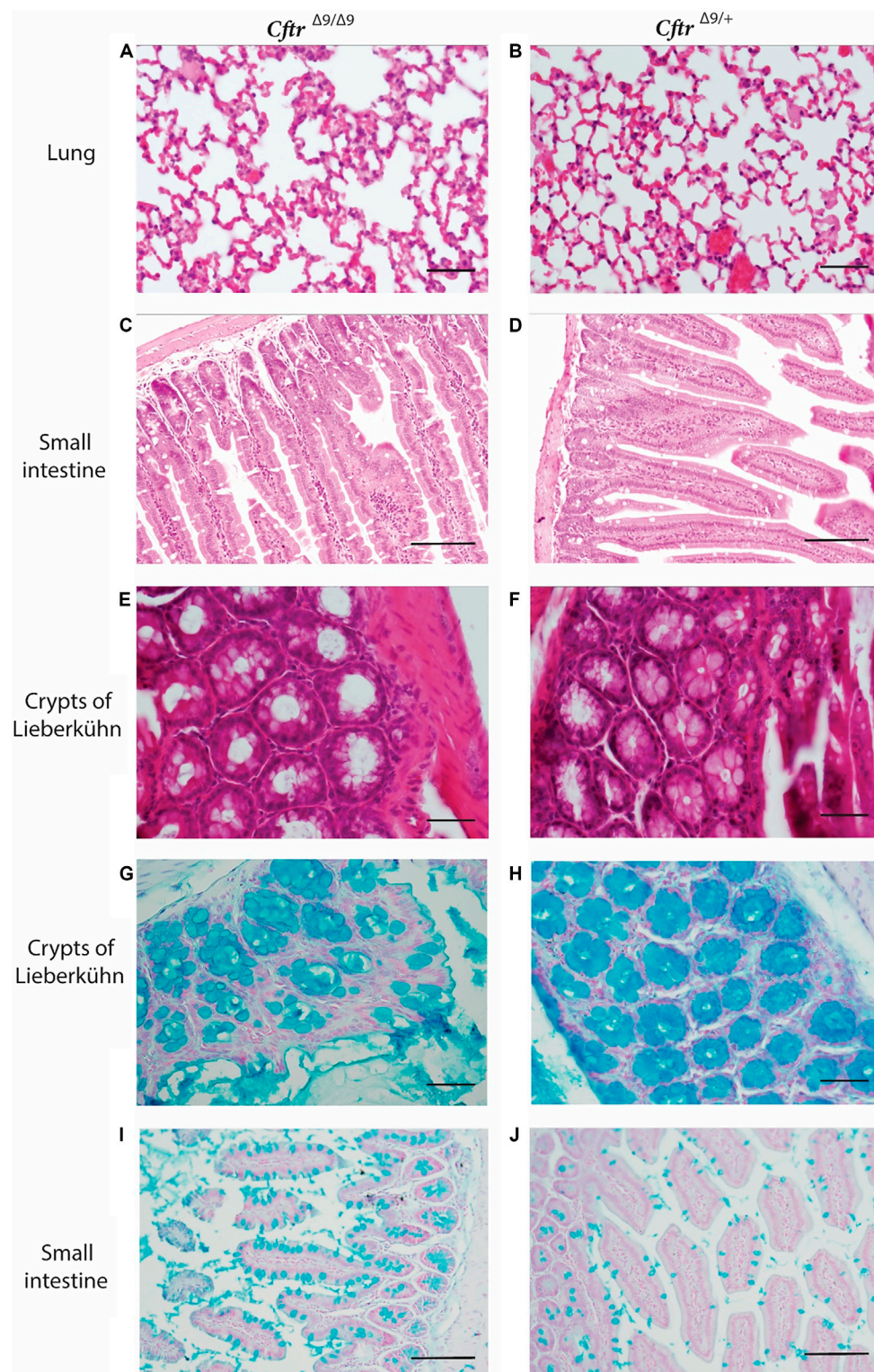
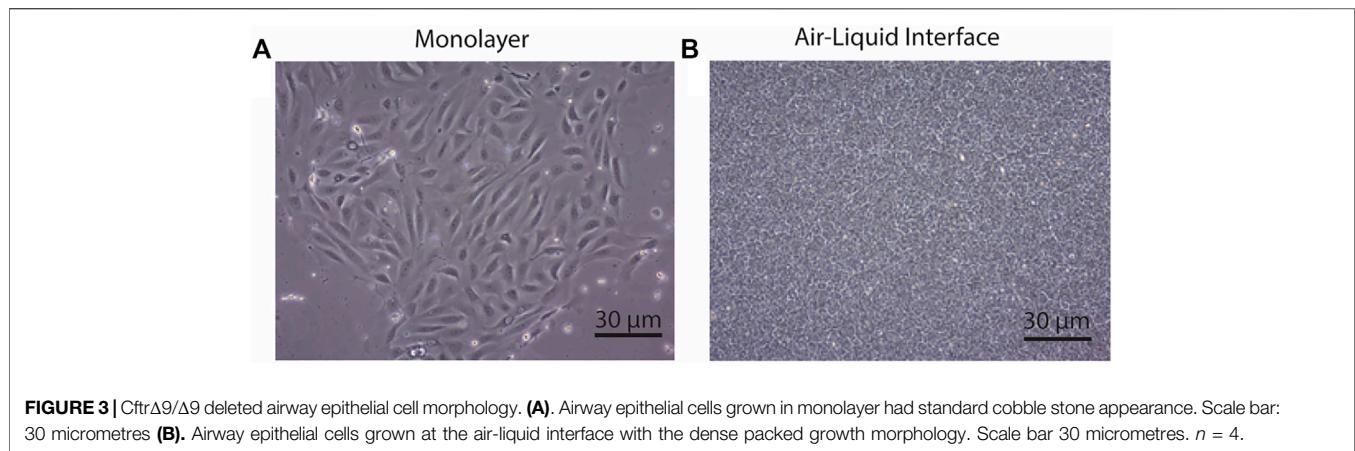


**FIGURE 2 |** Hematoxylin and Eosin and Alcian Blue staining of representative lung and intestinal sections from *Cftr*<sup>Δ9/Δ9</sup> and *Cftr*<sup>Δ9/+</sup> (control) mice. **(A–F)** Hematoxylin and Eosin stained **(A)**. Lung section for *Cftr*<sup>Δ9/Δ9</sup> mouse. **(B)**. Lung section for *Cftr*<sup>Δ9/+</sup> mouse. **(C)**. Small intestinal section from *Cftr*<sup>Δ9/Δ9</sup> mouse. **(D)**. Intestinal section from *Cftr*<sup>Δ9/+</sup> mouse. **(E)**. Crypts of Lieberkühn section from *Cftr*<sup>Δ9/Δ9</sup> mouse. **(F)**. Lieberkühn section from *Cftr*<sup>Δ9/+</sup> mouse. **(G–J)** Alcian blue stained **(G)**. a *Cftr*<sup>Δ9/Δ9</sup> mouse and **(H)**. *Cftr*<sup>Δ9/+</sup> mouse showing Crypts of Lieberkühn. Sections of small intestine from **(I)**. *Cftr*<sup>Δ9/Δ9</sup> mouse and **(J)**. *Cftr*<sup>Δ9/+</sup> mouse, showing goblet cells. *n* = 4. Images **(A,B)**, **(E–H)** were taken at  $\times 40$  (scale bar 20 micrometres) and **(C,D)**, **(I,J)** were taken at  $\times 20$  (scale bar 50 micrometres).



redundant, with *CFTR* exon 9 being identified. To investigate the *in vitro* and *in vivo* functionality of a CFTR isoform missing the domain encoded by exon 9, a *Cftr* $\Delta 9/\Delta 9$  mouse model was generated. Although *Cftr* mouse models do not develop CF lung disease, this model was used to ascertain if the level of disease severity correlated with *Cftr* genotype. It was hypothesised that mice lacking *Cftr* exon 9 alone would present with less severe pathological disease, when compared to other models, including *Cftr* gene KO or mutations resulting in premature termination of translation and nonsense mediated decay (Ratcliff et al., 1993; Colledge et al., 1995; Hasty et al., 1995). The *Cftr* $\Delta 9/\Delta 9$  mouse model generated here by homologous recombination presented with intestinal obstructions that were not prevented or improved by a liquid diet. At time of weaning (21 days) *Cftr* $\Delta 9/\Delta 9$  mice had a survival rate of 83% that dropped to 38% by day 50, with most mice eventually reaching a humane endpoint as described in the approved ethics protocol due to intestinal obstruction or malnutrition. Finally, airway epithelial cell cultures established from *Cftr* $\Delta 9/\Delta 9$  mouse airways were not responsive to the CFTR stimulator drug forskolin. Collectively, data generated in this study suggest that *Cftr* exon 9 is not partially redundant in mice, although airway cells from *Cftr* $\Delta 9/+$  littermates failed to culture due to contamination, poor adherence to the culture surface therefore this vital control group is lacking.

Survival of the *Cftr* $\Delta 9/\Delta 9$  mice generated here was initially high at 83% in the first 21 days, compared to the 21 days survival of published *Cftr* KO mouse models with no residual WT mRNA, such as the *Cftr* $^{tm1Unc}$  null model with ~25% survival (Snouwaert et al., 1992), and the *Cftr* $^{tm1Cam}$  null with only 17% (Ratcliff et al., 1993). *Cftr* mouse models with missense mutations and residual WT *Cftr* mRNA, such as *Cftr* $^{tm/Bay}$  has 40% and *Cftr* $^{tm/Hgu}$ , has 90% survival at 21 days. This could suggest that the disease severity of the *Cftr* $\Delta 9/\Delta 9$  mouse model generated here was marginally less severe with respect to intestinal complications. Homologous recombination mouse models as developed here, overcome any confounding issues by having no residual WT *Cftr* mRNA present that could potentially mitigate the disease presentation. As the *Cftr* exon 9 deletion occurred in the genome and is the only source of the *Cftr* gene expressed in this homozygous mouse model, there will be no residual

full-length *Cftr* that could influence the survival rate. In addition to specific genetic differences, variations in husbandry and housing environment such as the use of Peptamen<sup>®</sup> and ALPHA-dri<sup>®</sup> bedding as used here may also influence survival rates between mouse models.

There are many phenotypic differences between different mouse models of CF, due to background strain, environment and the specific *Cftr* mutation. Like many other animal models (e.g., the *mdx* mouse and Duchenne muscular dystrophy), CF mouse models do not accurately reflect the lung disease that occurs in humans, and our model was no different. Histological examination of organs from *Cftr* $\Delta 9/\Delta 9$  mice and heterozygous control littermates revealed few differences. There were no notable changes in the lungs, kidneys or liver evident on Hematoxylin and Eosin stained sections, which is comparable with many *Cftr* mouse models (Scholte et al., 2004). The organs, including the small intestines were also investigated for structural differences using Hematoxylin and Eosin staining of sections and examining mucus accumulation *via* Alcian blue staining. Examination of these sections from *Cftr* $\Delta 9/\Delta 9$  mice appeared to have an increase in the number of goblet cells with a swollen lumen and dilated Crypts of Lieberkühn, when compared to heterozygous littermates although quantification could not be done. Alcian blue staining showed dilated goblet cells and Crypts of Lieberkühn that were mucus filled. These findings reflect those from other CF mouse models presenting with intestinal complications and no lung disease (Wilke et al., 2011).

Airway epithelial cells were successfully isolated from homozygous *Cftr* $\Delta 9/\Delta 9$  mice and differentiated ALI cultures were established. The ALI cultures developed beating cilia, produced mucous and differentiated, as supported by high TEER values. Ussing chamber studies on ALI cultures revealed that these *Cftr* $\Delta 9/\Delta 9$  ALI cultures had a good response to amiloride, indicating sodium channels were present and blocked by the addition of this drug. The *Cftr* $\Delta 9/\Delta 9$  ALI cultures did not respond to forskolin stimulation, indicating that no CFTR channels were opening in response to the drug. There was minimal response to the CFTR inhibitor-172 as expected, and the small change seen could be due to volume-sensitive

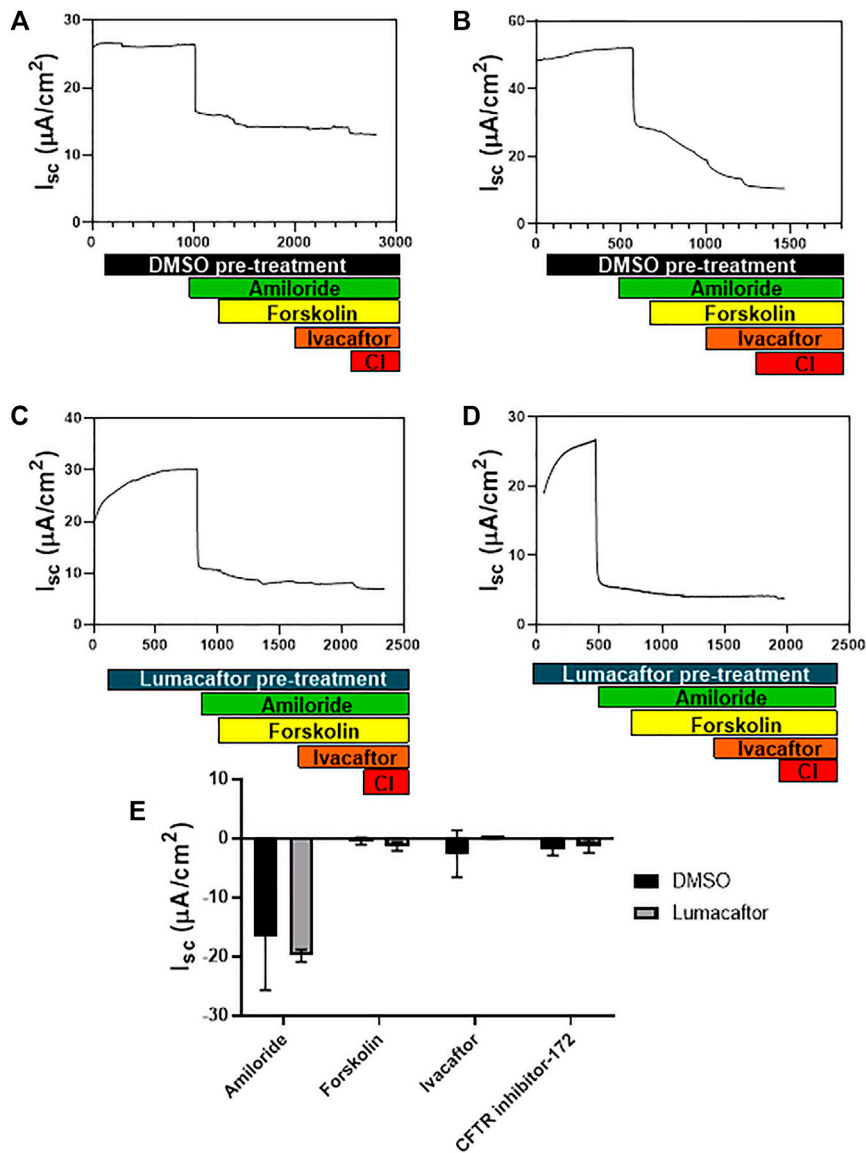


**FIGURE 4** | *Cftr*<sup>Δ9/Δ9</sup> epithelial cell CFTR function. **(A,B)**. Ussing chamber tracing showing change in short circuit current ( $I_{sc}$ ) in response to drug stimulation on *Cftr*<sup>Δ9/Δ9</sup> ALI cultures pre-treated for 24 h with DMSO. **(C,D)**. Ussing chamber tracing showing change in  $I_{sc}$  in response to drug stimulation on homozygote *Cftr* exon 9 deleted ALI cultures pre-treated for 24 h with Lumacaftor. **(E)**. Summary of changes in  $I_{sc}$  in response to amiloride, forskolin and CFTR inhibitor-172 for *Cftr*<sup>Δ9/Δ9</sup> ALI cultures pre-treated with DMSO (Black bars) or Lumacaftor (Grey bars) ( $I_{sc}$ ,  $n = 2$ ). Pre-treatment with DMSO (black bar) pre-treatment with Lumacaftor (blue bar), Amiloride addition (green bar), Forskolin stimulation (yellow bar), Ivacaftor stimulation (orange bar), CFTR inhibitor-172 (CI-red bar).

outwardly rectifying chloride ion conductance (Melis et al., 2014). These results indicate that the CFTR protein produced from the *Cftr* mRNA lacking exon 9 did not have the functional capacity to respond to forskolin, and therefore was a non-functional CFTR channel. When investigating this finding it was noted that electrophysiological responses differ depending on the mouse strain, since it is known that other factors such as genetic background can influence this response (Davidson and Rolfe 2001; Wilke et al., 2011). For example, *Cftr*<sup>tm1Cam</sup> C57Bl/6 mice have a forskolin response that is comparable to WT mice, whereas *Cftr*<sup>tm1Cam</sup> mice on an FVB background have no forskolin response (Wilke et al., 2011). The difference between

our *Cftr*<sup>Δ9/Δ9</sup> C57Bl/6 cell model lacking forskolin response and the *Cftr*<sup>tm1Cam</sup> C57Bl/6 model that had a forskolin response could be due to differences in the functional measurements. Here, pAEC ALI cultures were established *in vitro* from bronchial epithelium to measure the forskolin response, whereas Wilke et al (2011) utilised excised nasal epithelial sheets for Ussing chamber analysis (Wilke et al., 2011). This confounding issue reflects some of the problems encountered when utilising animal models to represent human disease and different methods to capture functional data.

Given the intermediate survival rate seen with diet supplemented (from 21 days) *Cftr*<sup>Δ9/Δ9</sup> mice, *Cftr* exon 9

could have some minor level of redundancy, at least in this mouse model. Duchenne muscular dystrophy is an example of genotype/phenotype correlations; and the *DMD* gene contains a number of partially dispensable exons, as we and others have observed some functional protein is preferable to no functional protein (Mann et al., 2001). This redundancy may be of therapeutic potential and future work should utilise human tissue to investigate this further. This mouse model like others could be used to bridge the gap between cell culture-based studies and human trials for evaluation of novel drug efficacy and dosing. This *Cftr*<sup>Δ9/Δ9</sup> mouse model demonstrates that exon skipping could be a feasible strategy for selected *CFTR* mutations to reduce a severe CF phenotype, although further investigation in human-derived tissue models is required as has been done for *CFTR* exon 23 skipping for mutations p.Trp1282X (Kim et al., 2022) (Oren et al., 2021; Michaels et al., 2022).

## DATA AVAILABILITY STATEMENT

The raw data supporting the conclusions of this article will be made available by the authors, without undue reservation.

## REFERENCES

- Clarke, L. L., Grubb, B. R., Yankaskas, J. R., Cotton, C. U., McKenzie, A., and Boucher, R. C. (1994). Relationship of a Non-cystic Fibrosis Transmembrane Conductance Regulator-Mediated Chloride Conductance to Organ-Level Disease in *Cftr*(-/-) Mice. *Proc. Natl. Acad. Sci. U S A* 91 (2), 479–483. doi:10.1073/pnas.91.2.479
- Colledge, W. H., Abella, B. S., Southern, K. W., Ratcliff, R., Jiang, C., Cheng, S. H., et al. (1995). Generation and Characterization of a delta F508 Cystic Fibrosis Mouse Model. *Nat. Genet.* 10 (4), 445–452. doi:10.1038/ng0895-445
- Cottart, C. H., Bonvin, E., Rey, C., Wendum, D., Bernaudin, J. F., Dumont, S., et al. (2007). Impact of Nutrition on Phenotype in *CFTR*-Deficient Mice. *Pediatr. Res.* 62 (5), 528–532. doi:10.1203/PDR.0b013e318155a61d
- Davidson, D. J., and Rolfe, M. (2001). Mouse Models of Cystic Fibrosis. *Trends Genet.* 17 (10), S29–S37. doi:10.1016/s0168-9525(01)02452-0
- Gaikwad, A., Khan, S., Kadam, S., Kadam, K., Dighe, V., Shah, R., et al. (2018). The *CFTR* Gene Mild Variants Poly-T, TG Repeats and M470V Detection in Indian Men with Congenital Bilateral Absence of Vas Deferens. *Andrologia* 50 (2), e12858. doi:10.1111/and.12858
- Gosselin, D., Stevenson, M. M., Cowley, E. A., Griesenbach, U., Eidelman, D. H., Boulé, M., et al. (1998). Impaired Ability of *Cftr* Knockout Mice to Control Lung Infection with *Pseudomonas aeruginosa*. *Am. J. Respir. Crit. Care Med.* 157 (4 Pt 1), 1253–1262. doi:10.1164/ajrccm.157.4.9702081
- Hasty, P., O'Neal, W. K., Liu, K. Q., Morris, A. P., Bebok, Z., Shumyatsky, G. B., et al. (1995). Severe Phenotype in Mice with Termination Mutation in Exon 2 of Cystic Fibrosis Gene. *Somat Cell Mol Genet* 21 (3), 177–187. doi:10.1007/BF02254769
- Henrie, A., Hemphill, S. E., Ruiz-Schultz, N., Cushman, B., DiStefano, M. T., Azzariti, D., et al. (2018). ClinVar Miner: Demonstrating Utility of a Web-Based Tool for Viewing and Filtering ClinVar Data. *Hum. Mutat.* 39 (8), 1051–1060. doi:10.1002/humu.23555
- Kim, Y. J., Sivetz, N., Layne, J., Voss, D. M., Yang, L., Zhang, Q., et al. (2022). Exon-skipping Antisense Oligonucleotides for Cystic Fibrosis Therapy. *Proc. Natl. Acad. Sci.* 119 (3), e2114858118. doi:10.1073/pnas.2114858118
- Koentgen, F., Lin, J., Katidou, M., Chang, L., Khan, M., Watts, J., et al. (2016). Exclusive Transmission of the Embryonic Stem Cell-Derived Genome through the Mouse Germline. *genesis* 54 (6), 326–333. doi:10.1002/dvg.22938

## ETHICS STATEMENT

The animal study was reviewed and approved by Murdoch University Animal ethics committee (Protocol ID: R3109/19).

## AUTHOR CONTRIBUTIONS

Conception of the study: SW Acquisition, analysis: KM, SF and RJ Drafting the article: KM Interpretation of histology: RJ Overall interpretation of data, revising manuscript critically: SW, SF, SS, and AK.

## ACKNOWLEDGMENTS

I would like to acknowledge that this project was funded by the United States CF Foundation (STICK15XX0), and the National Health and Medical Research Council of Australia (APP 1144791). AK is a Rothwell Family Fellow and SS is an NHMRC Practitioner Fellow. With thanks to Luke Berry for histological sample processing experience and Dr. Alex Larcombe for advice on sample collection.

- Lam, H. C., Choi, A. M., and Ryter, S. W. (2011). Isolation of Mouse Respiratory Epithelial Cells and Exposure to Experimental Cigarette Smoke at Air Liquid Interface. *J. Vis. Exp.* 48, 2513. doi:10.3791/2513
- Lavelle, G. M., White, M. M., Browne, N., McElvaney, N. G., and Reeves, E. P. (2016). Animal Models of Cystic Fibrosis Pathology: Phenotypic Parallels and Divergences. *Biomed. Res. Int.* 2016, 5258727. doi:10.1155/2016/5258727
- Li, H., Wen, Q., Li, H., Zhao, L., Zhang, X., Wang, J., et al. (2012). Mutations in the Cystic Fibrosis Transmembrane Conductance Regulator (*CFTR*) in Chinese Patients with Congenital Bilateral Absence of Vas Deferens. *J. Cyst Fibros* 11 (4), 316–323. doi:10.1016/j.jcf.2012.01.005
- Mann, C. J., Honeyman, K., Cheng, A. J., Ly, T., Lloyd, F., Fletcher, S., et al. (2001). Antisense-induced Exon Skipping and Synthesis of Dystrophin in the *Mdx* Mouse. *Proc. Natl. Acad. Sci. U S A* 98 (1), 42–47. doi:10.1073/pnas.011408598
- Martinovich, K. M., Iosifidis, T., Buckley, A. G., Looi, K., Ling, K. M., Sutanto, E. N., et al. (2017). Conditionally Reprogrammed Primary Airway Epithelial Cells Maintain Morphology, Lineage and Disease Specific Functional Characteristics. *Sci. Rep.* 7 (1), 17971. doi:10.1038/s41598-017-17952-4
- Melis, N., Tauc, M., Cougnon, M., Bendahhou, S., Giuliano, S., Rubera, I., et al. (2014). Revisiting *CFTR* Inhibition: a Comparative Study of *CFTRinh* -172 and GlyH-101 Inhibitors. *Br. J. Pharmacol.* 171 (15), 3716–3727. doi:10.1111/bph.12726
- Michaels, W. E., Pena-Rasgado, C., Kotaria, R., Bridges, R. J., and Hastings, M. L. (2022). Open reading Frame Correction Using Splice-Switching Antisense Oligonucleotides for the Treatment of Cystic Fibrosis. *Proc. Natl. Acad. Sci.* 119 (3), e2114886119. doi:10.1073/pnas.2114886119
- Molinski, S. V., Shahani, V. M., Subramanian, A. S., MacKinnon, S. S., Woollard, G., Laforet, M., et al. (2018). Comprehensive Mapping of Cystic Fibrosis Mutations to *CFTR* Protein Identifies Mutation Clusters and Molecular Docking Predicts Corrector Binding Site. *Proteins* 86 (8), 833–843. doi:10.1002/prot.25496
- O'Neal, W. K., Hasty, P., McCray, P. B., Jr, Casey, B., Rivera-Pérez, J., Welsh, M. J., et al. (1993). A Severe Phenotype in Mice with a Duplication of Exon 3 in the Cystic Fibrosis Locus. *Hum. Mol. Genet.* 2 (10), 1561–1569. doi:10.1093/hmg/2.10.1561
- Oren, Y. S., Avizur-Barchad, O., Ozeri-Galai, E., Elgrabli, R., Schirelman, M. R., Blinder, T., et al. (2021). Antisense Oligonucleotide Splicing Modulation as a Novel Cystic Fibrosis Therapeutic Approach for the W1282X Nonsense Mutation. *J. Cystic Fibrosis* S1569-1993, 02172. doi:10.1016/j.jcf.2021.12.012
- Radpour, R., Gourabi, H., Gilani, M. A., and Dizaj, A. V. (2007). Molecular Study of (TG)(M)(T)n Polymorphisms in Iranian Males with Congenital Bilateral

- Absence of the Vas Deferens. *J. Androl.* 28 (4), 541–547. doi:10.2164/jandrol.106.002337
- Ratcliff, R., Evans, M. J., Cuthbert, A. W., MacVinish, L. J., Foster, D., Anderson, J. R., et al. (1993). Production of a Severe Cystic Fibrosis Mutation in Mice by Gene Targeting. *Nat. Genet.* 4 (1), 35–41. doi:10.1038/ng0593-35
- Rozmahel, R., Wilschanski, M., Matin, A., Plyte, S., Oliver, M., Auerbach, W., et al. (1996). Modulation of Disease Severity in Cystic Fibrosis Transmembrane Conductance Regulator Deficient Mice by a Secondary Genetic Factor. *Nat. Genet.* 12 (3), 280–287. doi:10.1038/ng0396-280
- Scholte, B. J., Davidson, D. J., Wilke, M., and De Jonge, H. R. (2004). Animal Models of Cystic Fibrosis. *J. Cyst Fibros* 3 Suppl 2 (Suppl. 2), 183–190. doi:10.1016/j.jcf.2004.05.039
- Shteinberg, M., Downey, D. G., Beattie, D., McCaughan, J., Reid, A., Stein, N., et al. (2017). Lung Function and Disease Severity in Cystic Fibrosis Patients Heterozygous for p.Arg117His. *ERJ Open Res.* 3 (1), 00056–02016. doi:10.1183/23120541.00056-2016
- Snouwaert, J. N., Brigman, K. K., Latour, A. M., Malouf, N. N., Boucher, R. C., Smithies, O., et al. (1992). An Animal Model for Cystic Fibrosis Made by Gene Targeting. *Science* 257 (5073), 1083–1088. doi:10.1126/science.257.5073.1083
- Thomas, E. J., Gabriel, S. E., Makhlina, M., Hardy, S. P., and Lethem, M. I. (2000). Expression of Nucleotide-Regulated Cl(-) Currents in CF and normal Mouse Tracheal Epithelial Cell Lines. *Am. J. Physiol. Cell Physiol* 279 (5), C1578–C1586. doi:10.1152/ajpcell.2000.279.5.C1578
- Toronto, C. F. C. A. T. H. F. S. C. I. (2011). Cystic Fibrosis Mutation Database (CFTR1). Retrieved from <http://www.genet.sickkids.on.ca/>. (Accessed 22/08, 2020)
- Wilke, M., Buijs-Offerman, R. M., Aarbiou, J., Colledge, W. H., Sheppard, D. N., Touqui, L., et al. (2011). Mouse Models of Cystic Fibrosis: Phenotypic Analysis and Research Applications. *J. Cyst Fibros* 10 Suppl 2 (Suppl. 2), S152–S171. doi:10.1016/S1569-1993(11)60020-9
- Zeiber, B. G., Eichwald, E., Zabner, J., Smith, J. J., Puga, A. P., McCray, P. B., Jr., et al. (1995). A Mouse Model for the delta F508 Allele of Cystic Fibrosis. *J. Clin. Invest.* 96 (4), 2051–2064. doi:10.1172/JCI118253
- Zhou, Z., Duerr, J., Johannesson, B., Schubert, S. C., Treis, D., Harm, M., et al. (2011). The ENaC-Overexpressing Mouse as a Model of Cystic Fibrosis Lung Disease. *J. Cyst Fibros* 10 Suppl 2 (Suppl. 2), S172–S182. doi:10.1016/S1569-1993(11)60021-0

**Conflict of Interest:** The authors declare that the research was conducted in the absence of any commercial or financial relationships that could be construed as a potential conflict of interest.

**Publisher's Note:** All claims expressed in this article are solely those of the authors and do not necessarily represent those of their affiliated organizations, or those of the publisher, the editors and the reviewers. Any product that may be evaluated in this article, or claim that may be made by its manufacturer, is not guaranteed or endorsed by the publisher.

Copyright © 2022 Martinovich, Kicic, Stick, Johnsen, Fletcher and Wilton. This is an open-access article distributed under the terms of the Creative Commons Attribution License (CC BY). The use, distribution or reproduction in other forums is permitted, provided the original author(s) and the copyright owner(s) are credited and that the original publication in this journal is cited, in accordance with accepted academic practice. No use, distribution or reproduction is permitted which does not comply with these terms.